Design and Realization of GaN Trench Junction-Barrier-Schottky-Diodes

Wenshen Li, *Student Member, IEEE*, Kazuki Nomoto, *Member, IEEE*, Manyam Pilla, Ming Pan, Xiang Gao, Debdeep Jena, *Senior Member, IEEE*, and Huili Grace Xing, *Senior Member, IEEE*

***Abstract*— We present the design principle and experimental demonstrations of GaN trench junction-barrier-Schottky-diodes (trench JBSDs), where the Schottky contact within the patterned trenches is at the same plane as the adjacent p-n junctions. Assisted by the TCAD simulations, the leakage current reduction mechanism is identified as the reduced surface field (RESURF) effect due to the barrier-height difference between the p-n junction and Schottky junction. Design space for the width of stripe-shaped trenches is found to be <0.5 μm for a drift layer doping level of 10^{15}~10^{16} cm^{-3}, while for circular trenches, the size requirement is relaxed. In the fabricated devices with 1–4 μm diameter circular trenches, about 20 times reduction in the reverse leakage is observed with a characteristic shift in the turn-on voltage, which are signatures of the trench JBSD with desired RESURF. The experimental observations are in excellent agreement with the simulation results. This JBSD design shows promising potential in further improving the performance of Schottky-based GaN power devices without the need for ion-implantation or material regrowth.**

***Index Terms*— GaN, junction barrier Schottky, power electronics, reduced surface field (RESURF) effect, Schottky barrier diode (SBD), trench junction-barrier-Schottky-diode (trench JBSD), trench.**

I. Introduction

GaN holds great promises as a strong material for power electronics due to its superior Baliga's figure-of-merit (BV^2/R_{ON}) than SiC and Si. High power and high speed GaN lateral devices taking advantages of the high mobility 2-D electron gas in AlGaN/GaN heterostructure have seen rapid advancement in the past two decades [1]–[3], without the need for high quality bulk substrate. With the availability of low-dislocation-density bulk GaN substrates in recent years, vertical GaN power rectifiers with record high performance have been demonstrated in recent years [4]–[9], further showing the immense potential of GaN in the vertical device topology.

Among different types of GaN power rectifiers, GaN Schottky barrier diodes (SBDs) are shown to have the highest power efficiency in the breakdown voltage (BV) <1 kV range [10]. Although attractive, present GaN SBDs face the challenge in suppressing reverse leakage current, which is generally much higher than the GaN p-n diode (PND) and prevents the achievement of high BV. The device leakage can be dominated by point defects in the material. For example, carbon concentration is related to the leakage current in GaN SBDs and hopping transport of electrons assisted by carbon-related point defect states is hypothesized [11]. Another important source of the leakage inherent in the SBD structure is thermionic field emission through the thinned Schottky barrier at high field, which is shown to match well with the theoretical model [12].

In order to tackle the leakage current, improving material quality is the first step. In addition, ingenious device engineering can be employed. It is demonstrated that the incoorporation of a AlGaN tunneling layer on top of the SBD GaN drift layer could lower the reverse leakage while further reducing the turn-ON voltage [13]. Traditionally, junction-barrier-Schottky-diode (JBSD) structure proposed in [14] is widely used to reduce the reverse leakage. It combines the large BV of PNDs and the low turn-ON voltage of SBDs, enabling improved tradeoff between BV and R_{ON}. Successful demonstration of reliable and high blocking capability JBSDs have been reported in 4H-SiC [15], thanks to its mature ion implantation technology. Realization of conventional JBSDs in GaN, however, has been hindered by the difficulties in ion implantation and regrowth technologies, either of which can create the lateral p-n junction required in the JBSDs for reduced surface field (RESURF) under the Schottky contact [16]. In order to circumvent the issue, one can instead design trench patterns in p-GaN of a high-BV vertical PND [4]–[8], subsequently making Schottky contacts on the exposed n-GaN surface. In this JBSD structure, the Schottky contact surface is at the same plane as the p-n junction. Very recently, superior BV and simultaneously low R_{ON} were reported using a similar trench JBSD concept with designed edge terminations [17]. However, the RESURF effect could

Manuscript received December 5, 2016; revised January 13, 2017; accepted January 27, 2017. Date of publication February 21, 2017; date of current version March 22, 2017. This work was supported in part by the ARPA-E SWITCHES monitored by Tim Heidel and Isik Kizilyalli at the Cornell NanoScale Facility NSF under Grant ECCS-1542081. The review of this paper was arranged by Editor S. N. E. Madathil.

W. Li, K. Nomoto, D. Jena, and H. G. Xing are with the School of Electrical and Computer Engineering, Cornell University, Ithaca, NY 14850 USA (e-mail: wl552@cornell.edu; kn383@cornell.edu; djena@cornell.edu; grace.xing@cornell.edu).

M. Pilla is with Qorvo Inc., Richardson, TX 75080 USA (e-mail: Manyam.Pilla@qorvo.com).

M. Pan and X. Gao are with IQE RF LLC, Somerset, NJ 08873 USA (e-mail: mpan@iqep.com; xgao@iqep.com).

Color versions of one or more of the figures in this paper are available online at http://ieeexplore.ieee.org.

Digital Object Identifier 10.1109/TED.2017.2662702

0018-9383 © 2017 IEEE. Personal use is permitted, but republication/redistribution requires IEEE permission.
See http://www.ieee.org/publications_standards/publications/rights/index.html for more information.

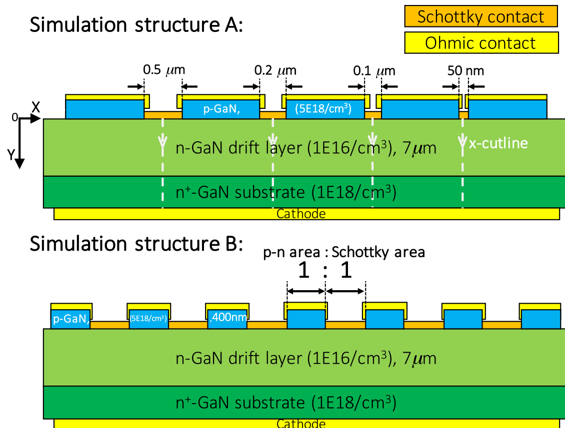

Fig. 1. Structures designed for simulation. Structure A (top) consists of stripe-shaped trenches with different widths. Shown in the schematic are trenches with width ranging from 0.5 μm to 50 nm. Trenches are separated by p-n junction area with much larger width than the trenches. Structure B (bottom) has alternating p-n and Schottky areas with a constant ratio of 1:1, while the trench size is varied from 1 μm to 50 nm.

not be explicitly confirmed, since the characteristic shift of the turn-ON voltage was not observed and the leakage behavior of the diodes was not reported. In this paper, we use simulations and experiments to present the design principle and leakage reduction mechanism in trench JBSDs.

II. SIMULATION

The device simulation is carried out using TCAD Sentaurus on two structures shown in Fig. 1. Structure A consists of stripe-shaped trenches of different widths ranging from 50 nm to 3 μm. The trenches are separated by p-n junctions with 8-μm width, which is designed to be much wider than the trenches, for the purpose of examining the possible RESURF effect under the Schottky contact within the trenches individually without interference from nearby trenches. Ohmic contacts are specified to the p-GaN top surface, which are electrically isolated from the Schottky contacts specified on the n-GaN surface within the trenches with a barrier height of 1 eV. The purpose of structure A is to investigate the critical dimension required for clear manifestation of the RESURF effect, which is enabled by the barrier height difference between Schottky junction inside the trench (~1 eV) and the p-n junction adjacent to the trench (~3 eV). Structure B consists of alternating p-n and Schottky junctions with a constant areal ratio of 1:1, while the width of the stripe-shaped trenches is varied from 50 nm to 0.5 μm in different simulation runs. With the 1:1 Schottky to p-n area ratio, the RESURF effect can be identified by comparing the average leakage current at reverse bias in devices with different trench widths. A "half-Schottky half-p-n" diode is also constructed as reference, whose current density is an average between a pure SBD and a pure PND. If a reduction of the average leakage current is observed for the structure B compared with the "half-Schottky half-p-n" diode, it would be due to the interaction between the Schottky junction and p-n junction. This interaction leads to the RESURF effect, as will be illustrated and explained in more details in Section IV. The nonlocal tunneling model in Sentaurus based on [18] is used to capture

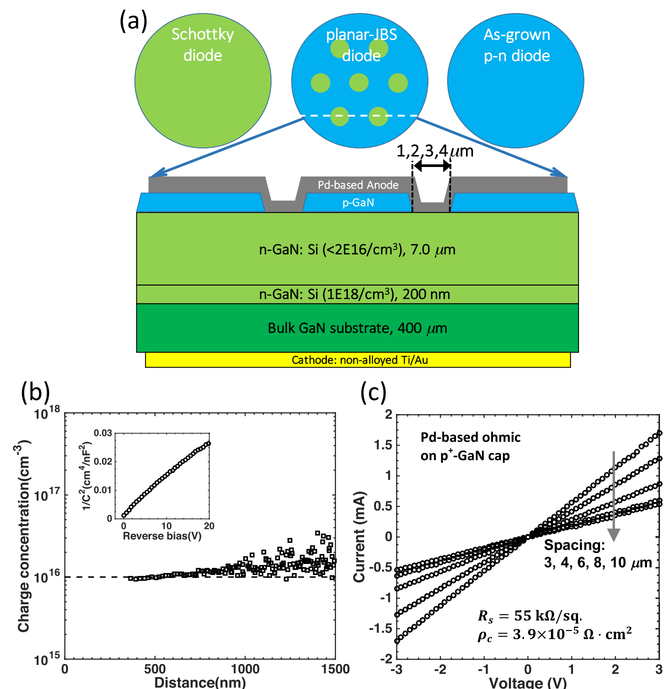

Fig. 2. (a) Schematic device top view and cross section of the fabricated trench JBSD. Circular trenches have a diameter of 1, 2, 3, and 4 μm. The total Schottky (trench) area is designed to be the same for each trench diameter. (b) Carrier concentration in the n-GaN drift layer extracted by the C–V measurement at 1 MHz. (c) Representative TLM I–V characteristics of the Pd-based ohmic contact on p-GaN. A low specific contact resistivity of 3.9×10^{-5} $\Omega \cdot \mathrm{cm}^2$ and p-GaN sheet resistance of 55 kΩ/sq. is extracted.

the dominant leakage mechanism through the Schottky barrier. In the nonlocal tunneling model, the tunneling probability is calculated self-consistently from the conduction band profile of the tunneling barrier using Wentzel–Kramers–Brillouin approximation.

III. EXPERIMENTS

As shown in Fig. 2(a), the trench JBSD epistructure is similar to our previous high-BV PNDs grown by Metal-Organic Chemical Vapour Deposition on freestanding GaN substrates with a threading dislocation density of $\sim 2 \times 10^6$ cm^{-2} [19]. A net doping concentration of $\sim 1 \times 10^{16}$ cm^{-3} in the drift layer is extracted by the capacitance-voltage (C–V) measurement [Fig. 2(b)]. Trench JBSDs are designed to have circular trench patterns with a diameter of 1, 2, 3, and 4 μm. For a better comparison between the trench JBSDs with different trench sizes, the total trench (i.e., Schottky) area in each diode is designed to be the same.

Although easier to simulate than the computationally expensive circular trench, the stripe-shaped trench requires submicrometer width for prominent RESURF effect (as will be shown in the later sections), thus is challenging to realize experimentally. On the other hand, the circular trench has a more uniform field profile along the trench periphery and is expected to have a relaxed size requirement due to the 3-D nature of its RESURF effect. Due to these considerations, we choose the more readily achievable circular trench design experimentally and compare the experimental results with the

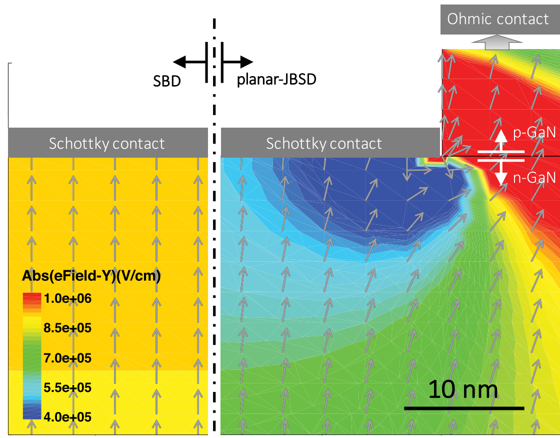

Fig. 3. Simulated electric field distribution at −200 V: (left) in a conventional Schottky diode and (right) in a trench JBSD with 50-nm trench width. The magnitude of the vertical electric field E_Y is represented by color, while the direction of the field is shown by gray arrows at representative grid points. The reduction in the vertical surface field (the RESURF effect) is clearly observed within the trench.

simulation using stripe-shaped trenches on the overall behavior and trend.

The trench JBSDs are fabricated by dry-etch first to form trenches and reveal the n-GaN surface, followed by deposition of circular Pd-based anodes. Pd forms an ohmic contact to p-GaN and a Schottky contact to n-GaN in the trench. Fig. 2(c) shows the representative transmission line method I–V characteristics of the ohmic contact on p-GaN. An excellent specific contact resistivity of $3.9 \times 10^{-5}\ \Omega \cdot \text{cm}^2$ is extracted. Conventional SBDs are made on the etched n-GaN surface. No additional field plate (FP) structures are used for edge termination, since the additional leakage often associated with the FP process [6] might mask the trend in the leakage current of trench JBSDs designed with varied trench sizes.

IV. Results and Discussion

In Fig. 3, the simulated electric field distribution at a reverse bias of −200 V is plotted for the 50-nm trench in Structure A, in comparison with a conventional SBD on the left. The magnitude of the vertical electric field E_Y is represented by color while the direction of the field is shown by gray arrows at representative grid points. It is clear from the color contrast that the vertical surface field within the trench is much reduced compared with the vertical surface field in the conventional SBD. Further inspection of the electric field direction reveals that the RESURF effect is due to the presence of the p-GaN at the edge of the trench. When forming contact with n-type GaN, the p-GaN has a higher barrier height (∼3 eV) than the Schottky contact metal (∼1 eV), thus part of the electrons in n-GaN under the Schottky contact metal are depleted by the adjacent p-GaN due to fringing effects. Consequently, the surface electric field arising from the resultant net positive charge under the Schottky contact terminates at the depletion region in the p-GaN instead of the Schottky contact, thus reducing the vertical component of the total surface field. In principle, this mechanism is the same as in the conventional JBSD, although the RESURF effect is weaker in the trench

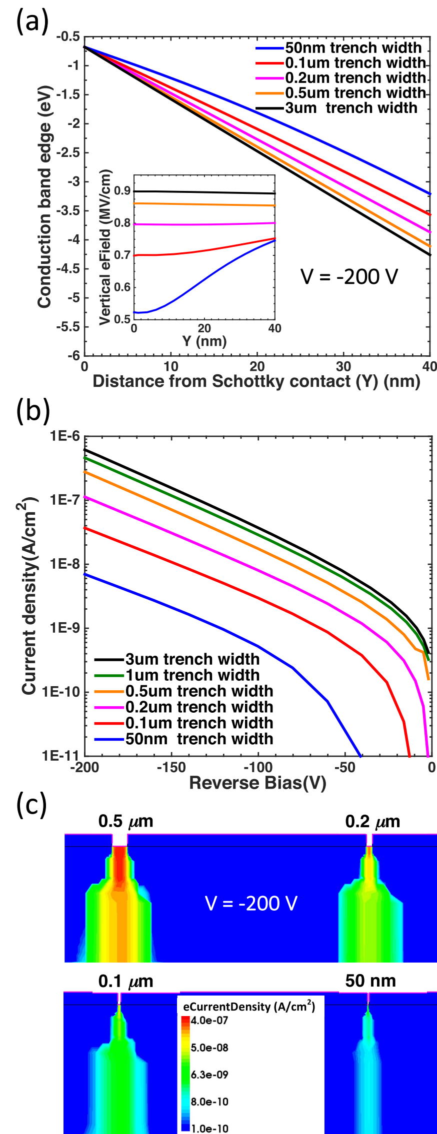

Fig. 4. Simulation results of structure A. (a) Conduction band edge distribution along the vertical x-cutlines (see Fig. 1) at −200 V. The inset shows the corresponding vertical electric field magnitude. (b) Reverse I–V characteristics of the Schottky trenches with different widths. Current is normalized by the corresponding Schottky contact area. (c) Electron current density distribution near the trench opening at a reverse voltage of 200 V.

JBSD devices due to the fact that the redirection of the electric field only happens near the device surface.

Fig. 4 shows the simulation results of structure A, which consists of stripe-shaped trenches of different widths. Fig. 4(a) (top) shows the conduction band profile at −200 V along the vertical cutlines centered in the stripe-shaped trenches (see Fig. 1). As the trench width reduces, the slope of the conduction band edge reduces, which corresponds to a reduced vertical surface electric field as shown in the inset. Compared with the 3-μm large trench where the RESURF effect is negligible at the center of the trench, the 50-nm small trench has ∼42% reduction in the vertical surface field. This reduction leads to a dramatic decrease in leakage current density due to the exponential dependence on the vertical

surface field as manifested in this simplified expression of the thermionic field emission process [12], [20]

$$J_{\mathrm{TFE}} = \frac{A^* T e \hbar E}{k} \times \sqrt{\frac{\pi}{2 m_n k T}} \times \exp\left[-\frac{1}{kT}\left(\phi_B - \frac{(e\hbar E)^2}{24 m_n (kT)^2}\right)\right]$$

where A^* is the effective Richardson constant and m_n is the electron effective mass in GaN. E is the vertical surface electric field at the metal–semiconductor interface. Note that this analytical expression is only valid in 1-D case thus not used in our simulation. Instead, a nonlocal tunneling model is employed as mentioned previously, which takes into count multiple tunneling paths and arbitrary barrier profile in the 2-D simulation. The reduction in leakage current density is identified in Fig. 4(b) where the current is normalized by the corresponding trench area. Close to two-orders of magnitude reduction in leakage current density is observe for the 50-nm trench width in comparison with the 3-μm trench width.

Fig. 4(c) shows the reverse current density distribution at −200 V near the trenches. As expected, the leakage current is primarily located near the trench region and arises from tunneling through the Schottky barrier. For trench widthes less than 0.5 μm, the leakage current density reduces dramatically. Again, close to two orders of magnitude reduction in the reverse current density through the Schottky barrier is observed for the 50-nm trench. The optimum design space for the *stripe-shaped* trench width is identified from Fig. 4(b) and (c) to be smaller than 0.5 μm for a doping level of 10^{16} cm^{-3}, in order to obtain a significant reduction in leakage current (>two times). A similar critical dimension of 0.5 μm is also observed for lower doping level of 10^{15} cm^{-3}. For *circular* trenches as employed in our experiments, the critical size is expected to be larger due to the 3-D nature of the RESURF effect in circular trenches.

Fig. 5 shows the simulated *I–V* characteristics of structure B, where a constant areal ratio of 1:1 is kept for the alternating p-n and Schottky junctions and only the trench size varies between different simulation runs. The average current density is calculated from dividing the total current by the total device area. Fig. 5(a) shows the forward *I–V* characteristics of the trench JBSDs in log scale, with conventional p-n and Schottky diodes included for comparison. As the trench width decreases, a shift of turn-ON voltage to a higher value is observed, which is also shown in the linear plot in Fig. 5(b). This shifting behavior of the turn-ON voltage is the characteristic of these JBSD-type devices and have been previously observed in conventional JBSDs [21], [22]. Fig. 5(c) shows the reverse current density. As expected, the PND has very low leakage current close to the precision limit of the simulation, and appears to be noisy. This is due to the absence of any nonideal leakage mechanisms in the simulation. On the contrary, conventional SBDs have much higher leakage current due to tunneling, reaching 1 μA/cm^2 at −200 V. The trench JBSDs have lower leakage than the SBDs. Compared with the reference "half-Schottky half-p-n" diode which averages the leakage current of PND and SBD, a reduction in the leakage current is observed for the trench JBSDs which gets more pronounced as the trench width reduces. Around approximately ten times leakage reduction is observed for the 0.1-μm case. Since the p-n and Schottky areas are the same, the reduction in the leakage current is due to the aforementioned interaction between the p-n junction and the Schottky junction, further confirming the RESURF effect in trench JBSDs.

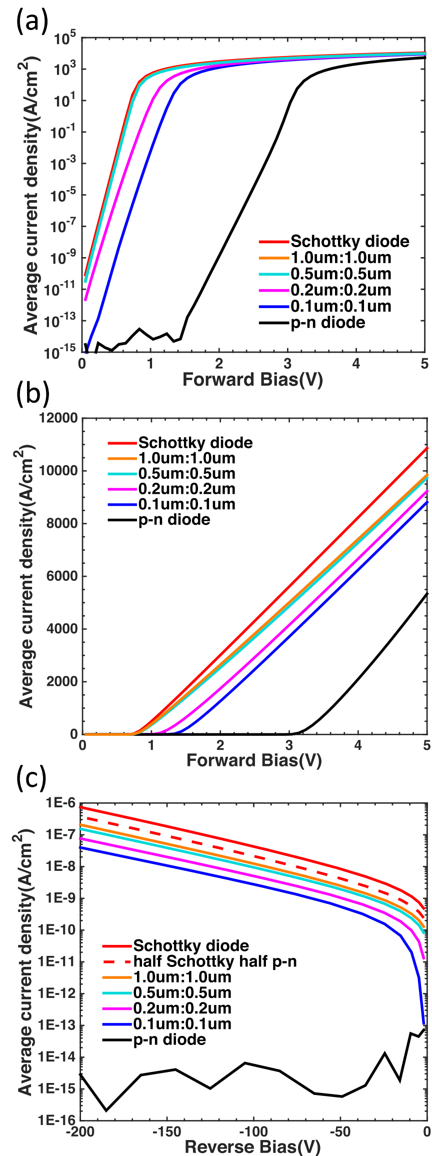

Fig. 5. Simulation results of structure B. (a)and (b) Forward and (c) reverse *I–V* characteristics. Currents flowing through the Schottky and PND area within the trench JBSDs are separately extracted. Average current density is calculated by normalizing the total current with the entire device area. Trench width varies from 1 to 0.1 μm while keeping a constant p-n and Schottky area ratio of 1:1. Conventional Schottky and PNDs are simulated for comparison, and the average of the two (half Schottky half p-n) is also shown in dashed line in (c).

Fig. 6 shows the measured *I–V* characteristics of the fabricated trench JBSDs. An ideal Schottky turn-ON behavior is observed for both trench JBSDs and the SBD at ∼1 V with an ideality factor of ∼1.00-1.05. A clear shift in the turn-ON voltage is observed in the log plot in Fig. 6(a) and highlighted in the inset, which agrees well with the simulation results [Fig. 5(a)]. The linear-scale *I–V* curves in Fig. 6(b) show

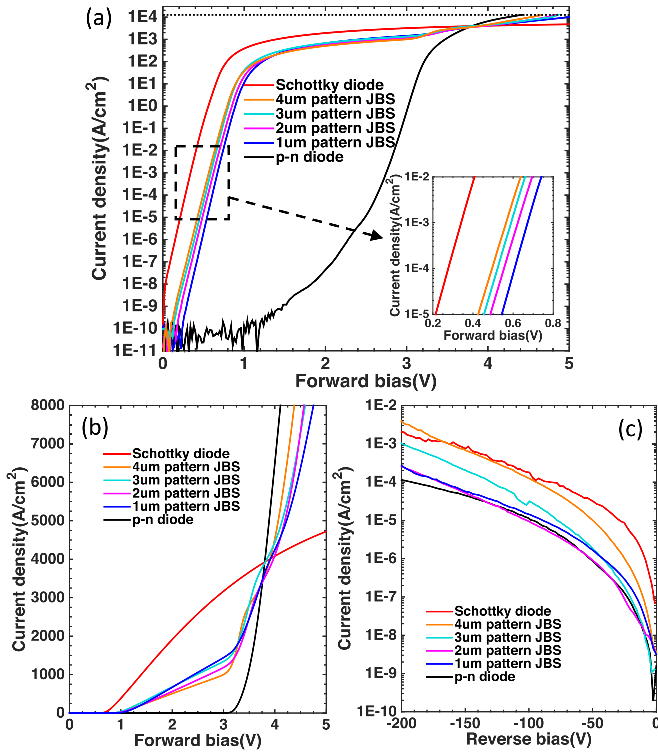

Fig. 6. Measured I–V characteristics of the trench JBSDs. All measured diodes have a diameter of 100 μm. (a) Forward I–V in log scale. An ideality factor of ~1–1.05 is extracted for the Schottky and trench JBS diodes. A clear trend of shifting in turn-on voltage is observed for JBSDs with different trench diameters, which agrees well with the simulation results [see Fig. 5(a)]. (b) Forward I–V in linear scale showing a characteristic two-step turn-on. (c) Reverse I–V in log scale. A clear trend of reduction in the reverse leakage is observed for the trench JBSDs over the range of 0~–200 V. The leakage in the PNDs seems to limit the leakage floor in this experiment, and the absolute value of leakage from experiments and simulations need to be further scrutinized.

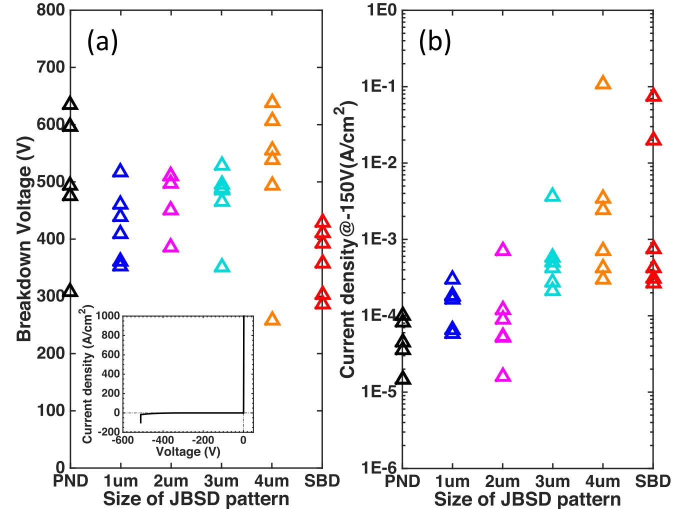

Fig. 7. (a) BV distribution and (b) reverse current density at −150 V for each type of measured devices. There are six devices for each type. Inset in (a) shows a representative I–V characteristic of the JBSDs, including the hard breakdown. The BV of all devices is determined by the device edge termination thus largely comparable. Given BV is not suitable to elucidate the RESURF effect in JBSDs, we scrutinize the trend in the reverse current density at lower voltages (b). The leakage is observed to reduce as the JBSD trench diameter reduces, which agrees well with the simulation [Fig. 5(c)].

a two-step turn-ON for the trench JBSDs, similar to [17]. The second turn-ON is due to the forward turn-ON of the p-n junction portion of the JBSDs. This is not captured in the simulated I–V curved in Fig. 5(b), mainly due to the much larger p-n to Schottky area ratio in the experimental devices as oppose to the 1:1 ratio in the simulation structure. The reverse I–V characteristics in Fig. 6(c) show a clear reduction of the leakage current density as the trench size decreases from 4 to 1 μm. Up to 20 times reduction in leakage current is achieved in the 1-μm trench JBSDs compared with conventional SBDs, reaching the PND leakage level. As the total trench area is designed to have the same total area, the reduction in leakage current is due to the RESURF effect arising from the trench JBSD design. In this particular batch of samples, the p-n junction leakage appears to be the limiting factor in further reducing the JBSD leakage, which can be improved in future work.

Fig. 7 shows the measured BV and the reverse current density at −150 V for various types of diodes. Since no FP is employed for the devices in this paper, the measured device BV is expected to be determined by the device edge termination. Optical microscope examination of the broken devices indeed confirms edge breakdown. As expected, the BV is comparable between as-grown PNDs and trench JBSDs, which all have mesa isolation. The BV for the SBD is a bit lower, possibly due to the severe edge field crowding at the anode metal edge. In this sense, the measured BV does not reflect the intrinsic BV achievable with optimized edge termination. On the other hand, it is observed from Fig. 7(b) that the leakage current density reduces as the trench JBSD trench size reduces, despite some scatter in the data, therefore the RESURF effect in the trench JBSD is confirmed. In addition, these experimental results corroborate with our expectation that the requirement on the trench size for circular pattern is relaxed compared with the case of stripe pattern adopted in the simulation (<0.5 μm). In GaN SBD devices with proper edge termination, the measured breakdown will largely be soft breakdown, which is determined by the leakage current and a pre-set current compliance. Thus, a reduction in leakage current of trench JBSD devices is expected to translate to higher achievable BV.

Finally, the benchmark plot of R_{ON}-BV is shown in Fig. 8. All the specific R_{ON} is calculated at $I_{\mathrm{ON}} = 100$ A/cm^2, in order to include the diode turn-ON effect. Along with the trench JBSD and the SBD obtained in this paper, the best-performing GaN SBDs in each category reported in [9], [23], and [24] are included. The figure-of-merit of the SBD and trench JBSD in this paper is comparable to that of the best SBD reported without FP. With FP structure, the recently reported trench JBSD out-performed the the best SBD with FP. However, the width of the reported stripe-shaped trench JBSD [17] is ~2 μm, which is larger than the requirement we obtained from simulation (<0.5 μm). Thus we speculate that the augmented BV observed in [17] is likely attributed to the reduced edge field instead of surface field due

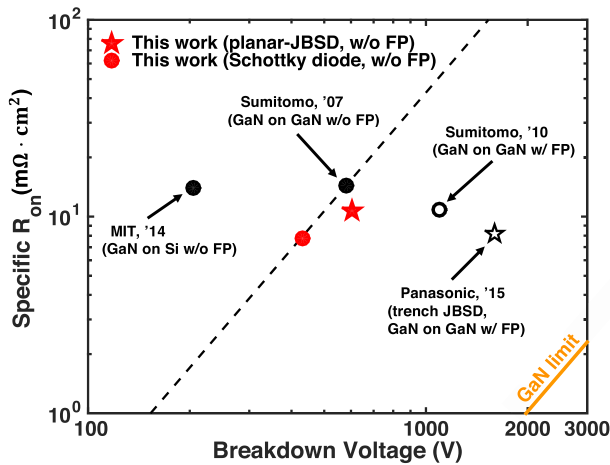

Fig. 8. Benchmark plot of BV versus specific R_{on}. Reference data points include the best vertical GaN SBDs reported in each category and the recently reported GaN trench JBSD [17]. All the R_{on} is calculated at $I_{on} = 100$ A/cm^2, including the diode turn-on effect. Hollow and filled symbols are for devices with and without FP, respectively.

to the adjacent p-n junction. Even better performance can be expected with <0.5 μm trench width together with optimized edge termination, taking advantage of the RESURF effect in the trench JBSD design.

V. Conclusion

Through device simulation and experiment, we investigated trench JBSD as an alternative GaN JBSD design which does not require formation of lateral p-n junction. We have elucidated the leakage reduction mechanism-RESURF effect in the GaN trench JBSD. The RESURF is due to the barrier height difference between the p-GaN and the Schottky metal, which causes the surface electric field under the Schottky metal to preferentially terminate at the p-GaN, thus reducing the vertical surface field component. We also identified the design space for such devices from simulation. For stripe-shaped trenches, the trench width is required to be smaller than 0.5 μm for a doping level of 10^{15}~10^{16} cm^{-3}, while in circular trenches, the size requirement is relaxed. We fabricated GaN trench JBSDs with different circular trench sizes from 4 to 1 μm and observed the signature shift in turn-ON voltage as well as ~20 times reduction in leakage current, both of which agree well with the simulation results. Circumventing the current technological difficulties in creating lateral p-n junction, the trench JBSD design offers promising opportunity for further improvement of the performance of Schottky-based GaN power devices.

References

[1] H. Xing, Y. Dora, A. Chini, S. Heikman, S. Keller, and U. K. Mishra, "High breakdown voltage AlGaN-GaN HEMTs achieved by multiple field plates," *IEEE Electron Device Lett.*, vol. 25, no. 4, pp. 161–163, Apr. 2004.

[2] S. L. Selvaraj, A. Watanabe, A. Wakejima, and T. Egawa, "1.4-kV breakdown voltage for AlGaN/GaN high-electron-mobility transistors on silicon substrate," *IEEE Electron Device Lett.*, vol. 33, no. 10, pp. 1375–1377, Oct. 2012.

[3] E. Bahat-Treidel *et al.*, "Fast-switching GaN-based lateral power Schottky barrier diodes with low onset voltage and strong reverse blocking," *IEEE Electron Device Lett.*, vol. 33, no. 3, pp. 357–359, Mar. 2012, doi: 10.1109/LED.2011.2179281.

[4] I. Kizilyalli, T. Prunty, and O. Aktas, "4-kV and 2.8-mΩ-cm^2 vertical GaN p-n diodes with low leakage currents," *IEEE Electron Device Lett.*, vol. 36, no. 10, pp. 1073–1075, Oct. 2015.

[5] K. Nomoto *et al.*, "GaN-on-GaN p-n power diodes with 3.48 kV and 0.95 mΩ-cm^2: A record high figure-of-merit of 12.8 GW/cm^2," in *IEDM Tech. Dig.*, Dec. 2015, pp. 7–9.

[6] K. Nomoto *et al.*, "1.7-kV and 0.55-mΩ-cm^2 GaN p-n diodes on bulk GaN substrates with avalanche capability," *IEEE Electron Device Lett.*, vol. 37, no. 2, pp. 161–164, Feb. 2016.

[7] H. Ohta *et al.*, "Vertical GaN p-n junction diodes with high breakdown voltages over 4 kV," *IEEE Electron Device Lett.*, vol. 36, no. 11, pp. 1180–1182, Nov. 2015. [Online]. Available: http://dx.doi.org/10.1109/LED.2015.2478907

[8] A. M. Armstrong *et al.*, "High voltage and high current density vertical GaN power diodes," *Electron. Lett.*, vol. 52, no. 13, pp. 1170–1171, 2016.

[9] Y. Saitoh *et al.*, "Extremely low on-resistance and high breakdown voltage observed in vertical GaN Schottky barrier diodes with high-mobility drift layers on low-dislocation-density GaN substrates," *Appl. Phys. Exp.*, vol. 3, no. 8, p. 081001, 2010.

[10] S. Chowdhury and T. P. Chow, "Comparative performance assessment of SiC and GaN power rectifier technologies," *Phys. Status-Solidi C*, vol. 13, nos. 5–6, pp. 360–364, 2016.

[11] Y. Cao, R. Chu, R. Li, M. Chen, R. Chang, and B. Hughes, "High-voltage vertical GaN Schottky diode enabled by low-carbon metal-organic chemical vapor deposition growth," *Appl. Phys. Lett.*, vol. 108, no. 6, p. 062103, 2016.

[12] J. Suda *et al.*, "Nearly ideal current–voltage characteristics of Schottky barrier diodes formed on hydride-vapor-phase-epitaxy-grown GaN free-standing substrates," *Appl. Phys. Exp.*, vol. 3, no. 10, p. 101003, 2010.

[13] Y. Cao, R. Chu, R. Li, M. Chen, and A. Williams, "Improved performance in vertical GaN Schottky diode assisted by AlGaN tunneling barrier," *Appl. Phys. Lett.*, vol. 108, no. 11, p. 112101, 2016.

[14] B. J. Baliga, "The pinch rectifier: A low-forward-drop high-speed power diode," *IEEE Electron Device Lett.*, vol. 5, no. 6, pp. 194–196, Jun. 1984.

[15] B. A. Hull *et al.*, "Performance and stability of large-area 4H-SiC 10-kV junction barrier Schottky rectifiers," *IEEE Trans. Electron Devices*, vol. 55, no. 8, pp. 1864–1870, Aug. 2008.

[16] J. A. Appels and H. M. J. Vaes, "High voltage thin layer devices (RESURF devices)," in *IEDM Tech. Dig.*, vol. 25. Dec. 1979, pp. 238–241.

[17] K. Ryo *et al.*, "A high current operation in a 1.6 kV GaN-based trench hybrid-junction diode (THD)," IEICE, Japan, Tech. Rep. ED2015-75, vol. 115, no. 329, pp. 39–42, 2015.

[18] M. Ieong, P. M. Solomon, S. Laux, H.-S. Wong, and D. Chidambarrao, "Comparison of raised and Schottky source/drain MOSFETs using a novel tunneling contact model," in *IEDM Tech. Dig.*, Jun. 1998, pp. 733–736.

[19] Z. Hu *et al.*, "Near unity ideality factor and Shockley-read-Hall lifetime in GaN-on-GaN pn diodes with avalanche breakdown," *Appl. Phys. Lett.*, vol. 107, no. 24, p. 243501, 2015.

[20] F. A. Padovani and R. Stratton, "Field and thermionic-field emission in Schottky barriers," *Solid-State Electron.*, vol. 9, no. 7, pp. 695–707, 1966.

[21] F. Dahlquist, J. Svedberg, C. M. Zetterling, M. Östling, B. Breitholtz, and H. Lendenmann, "A 2.8 kV, forward drop JBS diode with low leakage," *Mater. Sci. Forum*, vol. 338, pp. 1179–1182, May 2000.

[22] C. Feng-Ping, Z. Yu-Ming, L. Hong-Liang, Z. Yi-Men, and H. Jian-Hua, "Study of 4H-SiC junction barrier Schottky diode using field guard ring termination," *Chin. Phys. B*, vol. 19, no. 9, p. 097107, 2010.

[23] S. Hashimoto, Y. Yoshizumi, T. Tanabe, and M. Kiyama, "High-purity GaN epitaxial layers for power devices on low-dislocation-density GaN substrates," *J. Cryst. Growth*, vol. 298, pp. 871–874, Jan. 2007.

[24] Y. Zhang *et al.*, "GaN-on-Si vertical Schottky and p-n diodes," *IEEE Electron Device Lett.*, vol. 35, no. 6, pp. 618–620, Jun. 2014.

Wenshen Li (S'16) received the B.S. degree in microelectronics from Tsinghua University, Beijing, China, in 2015. He is currently pursuing the Ph.D. degree in electrical engineering with Cornell University, Ithaca, NY, USA.

His current research interests include GaN high-speed and high-power devices.

Kazuki Nomoto (M'11) received the B.S., M.S., and Ph.D. degrees in electrical engineering from Hosei university, Tokyo, Japan in 2009. He was a Postdoctoral Research Associate from 2012 to 2015 at Department of Electrical Engineering, University of Notre Dame, IN.

He has been working at School of Electrical and Computer Engineering, Cornell University, NY since 2015, he has been engaged in the research and development of wide bandgap semiconductor power devices.

Manyam Pilla, photograph and biography not available at the time of publication.

Ming Pan, photograph and biography not available at the time of publication.

Xiang Gao, photograph and biography not available at the time of publication.

Debdeep Jena (M'03–SM'14) received the B.Tech. degree in electrical engineering from the IIT, Kanpur, India, in 1998, and the Ph.D. degree in electrical and computer engineering from the University of California, Santa Barbara, CA, USA, in 2003.

He is currently a Professor in the School of Electrical and Computer Engineering and the Department of Materials Science and Engineering, Cornell University, Ithaca, NY, USA.

Huili Grace Xing (S'01–M'03–SM'14) received the B.S. degree in physics from Peking University, Beijing, China, in 1996, the M.S. degree in material science from Lehigh University, Bethlehem, PA, USA, in 1998, and the Ph.D. degree in electrical engineering from the University of California, Santa Barbara, CA, USA, in 2003.

She is currently a Professor in the School of Electrical and Computer Engineering and the Department of Materials Science and Engineering, Cornell University, Ithaca, NY, USA.